ChemPubSoc Europe

DOI: 10.1002/chem.201602047

CHEMISTRY A European Journal Full Paper

Glycoclusters

Toward the Rational Design of Galactosylated Glycoclusters That Target *Pseudomonas aeruginosa* Lectin A (LecA): Influence of Linker Arms That Lead to Low-Nanomolar Multivalent Ligands

Shuai Wang[+],[a] Lucie Dupin[+],[b] Mathieu Noël,[c] Cindy J. Carroux,[a] Louis Renaud,[d] Thomas Géhin,[b] Albert Meyer,[c] Eliane Souteyrand,[b] Jean-Jacques Vasseur,[c] Gérard Vergoten,[e] Yann Chevolot,*[b] François Morvan,*[c] and Sébastien Vidal*[a]

Abstract: Anti-infectious strategies against pathogen infections can be achieved through antiadhesive strategies by using multivalent ligands of bacterial virulence factors. LecA and LecB are lectins of *Pseudomonas aeruginosa* implicated in biofilm formation. A series of 27 LecA-targeting glycoclusters have been synthesized. Nine aromatic galactose aglycons were investigated with three different linker arms that connect the central mannopyranoside core. A low-nanomolar ($K_d = 19$ nM, microarray) ligand with a tyrosine-based linker arm could be identified in a structure–activity relationship study. Molecular modeling of the glycoclusters bound to the lectin tetramer was also used to rationalize the binding properties observed.

Introduction

Bacterial adhesion at the cell surface takes place through multivalent protein–carbohydrate interactions between the bacterial proteins (e.g., toxins, adhesins, and lectins) and the glycoconjugates at the outer cell membrane (e.g., glycolipids and glycoproteins).[1] High avidity is achieved through multivalency by presenting multiple copies of the oligosaccharidic partner at the malleable cell surface and also by the multimeric character of most bacterial lectins. The design of synthetic analogues of oligosaccharides has been largely studied by chemists[2,3] and has now provided interesting results in antiadhesive therapy against bacterial infections that target, for instance, *Escherichia coli*[4–8] or *Pseudomonas aeruginosa*.[9–14] LecA and LecB are two soluble tetrameric lectins of *Pseudomonas aeruginosa* implicated in biofilm formation.[15] Although LecA binds preferentially to galactosides,[16] fucosides are recognized by LecB.[17]

The main part of the design of multivalent architectures that display multiple carbohydrate copies on their periphery is the choice of the central-core scaffold. The correct balance between valency and density is required to avoid, on one hand, low valency and poor affinity, but also, on the other hand, high valency and steric hindrance toward the protein-binding partners and hence poor efficacy in this context. The geometry of the scaffolds also plays a role in the affinity toward lectins.[18] Synthetic glycoclusters have been designed based on diverse aromatic-core scaffolds, such as porphyrins,[2,19–23] fullerenes,[2,24–28] calixarenes,[2,9,21,29–32] and more recently pillararenes.[33–37] Oligonucleotide chemistry with the powerful phosphoramidite coupling offers a general and accessible platform for the design of multivalent glycoclusters because valency can be easily modulated as well as the overall geometry of the macromolecule with optimal water solubility thanks to the phosphodiester groups.[14,38–44] In this context, a tetravalent mannopyranoside core platform was also introduced and provided glycoclusters of high affinity toward LecA as antibacterial candidates.[14,43,45,46]

The type of linker used to connect the carbohydrate to the core also greatly affects the binding properties toward lectins. The present study focuses on the design of LecA high-affinity

[a] Dr. S. Wang,[+] C. J. Carroux, Dr. S. Vidal
Institut de Chimie et Biochimie Moléculaires et Supramoléculaires
Laboratoire de Chimie Organique 2 - Glycochimie UMR 5246
CNRS - Université Claude Bernard Lyon 1
43 Boulevard du 11 Novembre 1918, 69622 Villeurbanne (France)
E-mail: sebastien.vidal@univ-lyon1.fr

[b] L. Dupin,[+] Dr. T. Géhin, Dr. E. Souteyrand, Dr. Y. Chevolot
Institut des Nanotechnologies de Lyon (INL) - UMR CNRS 5270
Ecole Centrale de Lyon, Université de Lyon
36 Avenue Guy de Collongue, 69134 Ecully cedex (France)
E-mail: yann.chevolot@ec-lyon.fr

[c] M. Noël, A. Meyer, Dr. J.-J. Vasseur, Dr. F. Morvan
Institut des Biomolécules Max Mousseron (IBMM) - UMR 5247
CNRS - Université Montpellier - ENSCM
Place Eugène Bataillon, CC1704, 34095 Montpellier cedex 5 (France)
E-mail: morvan@univ-montp2.fr

[d] Dr. L. Renaud
Institut des Nanotechnologies de Lyon, UMR CNRS 5270
Université Claude Bernard Lyon 1, Université de Lyon
43 Boulevard du 11 Novembre 1918, 69622 Villeurbanne (France)

[e] Dr. G. Vergoten
Unité de Glycobiologie Structurale et Fonctionnelle (UGSF) - UMR 8576
CNRS - Université de Lille 1, Cité Scientifique, Avenue Mendeleiev
Bat C9, 59655 Villeneuve d'Ascq cedex (France)

[+] These authors contributed equally to this work.

Supporting information for this article is available on the WWW under http://dx.doi.org/10.1002/chem.201602047.

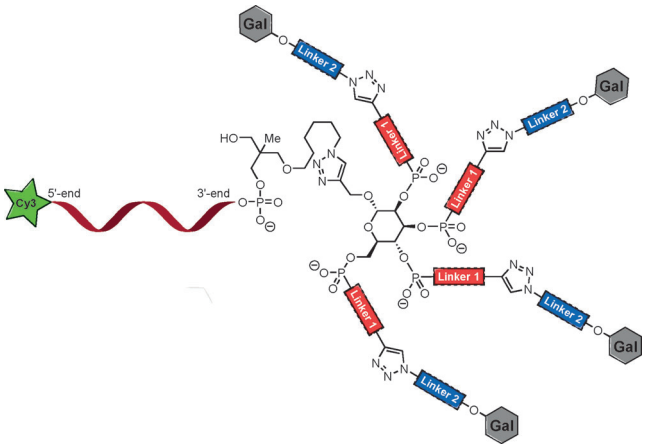

Figure 1. General structure of mannose-centered glycoclusters.

glycoclusters based on phosphoramidite coupling with particular insight into the influence of two linker arms (**Linker 1** and **Linker 2**; Figure 1) used in the glycocluster architecture. **Linker 1** is directly connected to the mannopyranoside core scaffold, whereas **Linker 2** is connected to the carbohydrate epitope (i.e., galactoside) with a triazole moiety that conjugates both linkers. The mannose unit used as the tetravalent-core scaffold was selected as the best candidate among several other saccharides from earlier studies.[38,43,45] A cyanine fluorescent-dye (Cy3)-labeled 15-mer oligonucleotide sequence was introduced for multiplexing on carbohydrate microarrays,[47] thus allowing rapid qualitative and quantitative[41] screening of the LecA-binding properties.

The influence of **Linker 1** was studied by using three different linkers of increasing lengths: propyl (Pro), diethyleneglycolmethylene (EG_2M), and triethyleneglycolmethylene (EG_3M). Access to the carbohydrate epitopes by the lectin moiety is crucial for optimal binding properties; that is, the shorter **Linker 1** is, the poorer the affinity is to be expected.

The nature of the aglycon moiety at the anomeric position of the galactosides has been carefully studied, and aromatic derivatives have displayed improved binding properties for the lectin.[3,13,31,43,46,48–51] The present study provides a new set of nine potential aromatic linkers (**Linker 2**; Figure 1) with phenyl, furanyl, thiophenyl, pyridinyl, or tyrosinyl groups. The influence of the distance to the anomeric carbon atom and the heteroaromatic structures is discussed.

After synthetic efforts toward the carbohydrate building blocks and conjugation to the oligonucleotide scaffolds, a series of 27 glycoclusters were evaluated by means of DNA-directed immobilized (DDI) carbohydrate microarrays to assess their binding properties toward LecA. The results obtained were rationalized by using molecular-modeling studies for the best ligands identified through their structure–activity relationships.

Results and Discussion

The binding pocket of LecA exhibits a preference for aromatic aglycons with additional interactions through CH–π stacking with the histidine (His) residue His50.[48] This type of study emerged with the design of a *C*-galactoside[51] with an aromatic moiety that displayed low-micromolar dissociation constants, as measured by using isothermal titration calorimetry (ITC; Table 1). Based on the known micromolar affinity of *para*-nitrophenyl β-D-galactoside ($K_d = 140$ μM), we designed an analogue in which the nitro functionality was replaced by an azidoacetamido group[31] as a reactive handle for conjugation to multivalent core platforms. Similarly, the aromatic aglycon reported by Reymond and co-workers displayed improved binding properties toward LecA.[13] Further studies by the same group identified larger aromatic aglycons, such as 2-naphthyl, as promising targets,[48] along with the corresponding thioglycoside.[49] Meanwhile, other reports have used multivalent glycoclusters with aromatic aglycons in their linker arm. Improved binding properties toward LecA were demonstrated when conjugated to modified oligonucleotides and by using a carbohydrate-microarray system for the screening of affinity.[43,46]

Table 1. Aromatic aglycons investigated for improved LecA-binding properties.

Galactoside	K_d [μM][a]	Number tested[b]	Authors
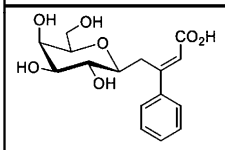	37	10	Chabre et al.[51]
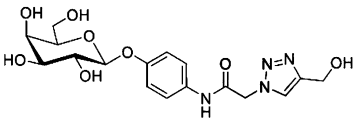	5.8	0	Cecioni et al.[31]
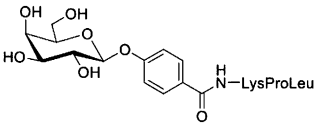	4.2	11	Kadam et al.[13]
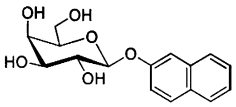	4.2	11	Kadam et al.[48]
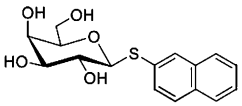	6.3	2	Rodrigue et al.[49]

[a] The K_d values were measured by using ITC. [b] Number of additional aromatic aglycons tested within the study and for which the best ligand identified is presented herein.

Synthesis of the azido-functionalized carbohydrates

Introduction of a glycol moiety between the aromatic ring and the anomeric carbon atom (Scheme 1) was achieved by galactosylation of nitrophenoxyethanols **2a–c** readily obtained by alkylation from ethylene carbonate of the corresponding phenols **1a–c**.[52–54] Galactosides **3a–c** were converted into the de-

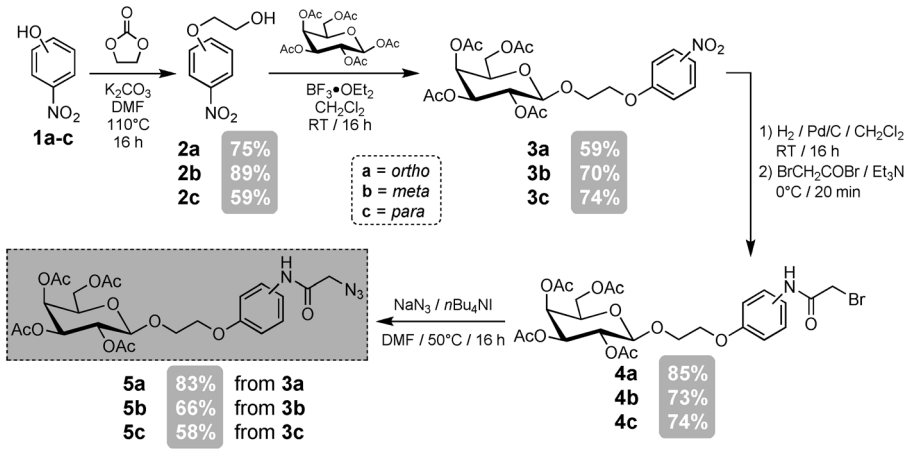

Scheme 1. Synthesis of ethyleneglycol-phenyl-azidoacetamido galactosides GalEG*o*-PhNAz (**5a**), GalEG*m*-PhNAz (**5b**), and GalEG*p*-PhNAz (**5c**; Gal = galactose).

sired azido-functionalized carbohydrates **5a–c** through the bromo intermediates **4a–c**.[31] This three-step process from the nitro to the azidoacetamido (**3a–c**→**5a–c**) moiety was interrupted when the bromo derivatives **4a–c** were obtained by rapid column chromatography on silica gel, thus obtaining optimal yields for the final azidation step.

Furan-2,5-dicarboxylic acid (**6**) was diesterified to dimethylester **7**[55] and selectively monoreduced to the corresponding alcohol **8** (Scheme 2). Galactosylation afforded the desired β-anomer **9**. Saponification under smooth conditions to the carboxylic acid intermediate, followed by condensation with 2-(2-azidoethoxy)ethanamine and re-acetylation of the crude mixture afforded the furan-based galactoside **10**.

A similar synthetic strategy was adopted toward the thiophen-based linker arm (Scheme 3). Dicarboxylic acid **11** was converted into dimethylester **12** and selective mono-saponification to acid/ester **13** followed by chemoselective reduction of the carboxylic acid afforded alcohol **14**. Galactosylation was

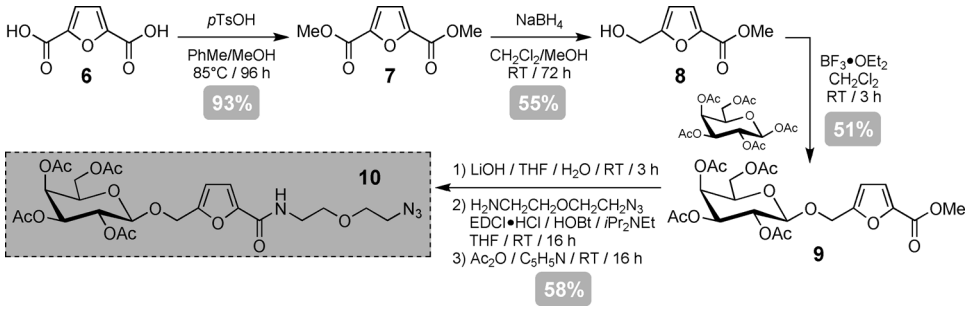

Scheme 2. Synthesis of the furan-based galactosides GalFurEG$_2$N$_3$ (**10**; fur = furanyl). EDCI = 1-ethyl-3-(3-dimethylaminopropyl)carbodiimide, HOBt = 1-hydroxybenzotriazole, TsOH = toluenesulfonic acid.

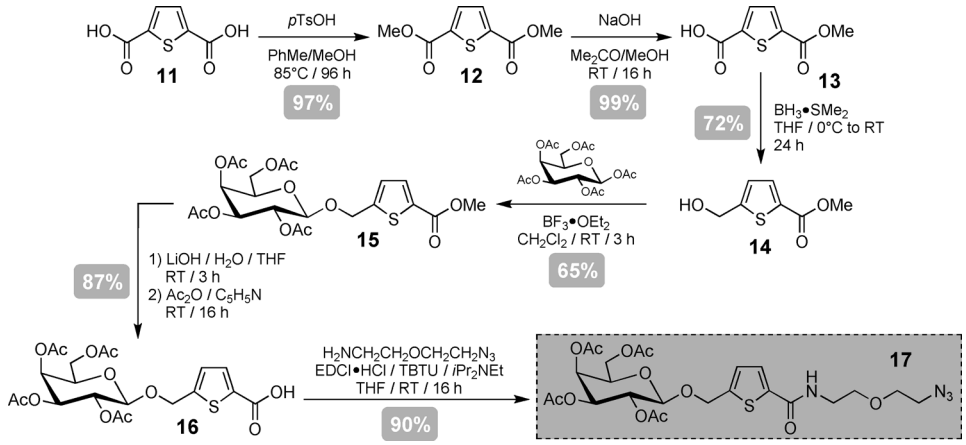

Scheme 3. Synthesis of the thiophen-based galactosides GalThioEG$_2$N$_3$ (**17**; Thio = thiophenyl). TBTU = 2-(1*H*-benzotriazole-1-yl)-1,1,3,3-tetramethyluronium tetrafluoroborate.

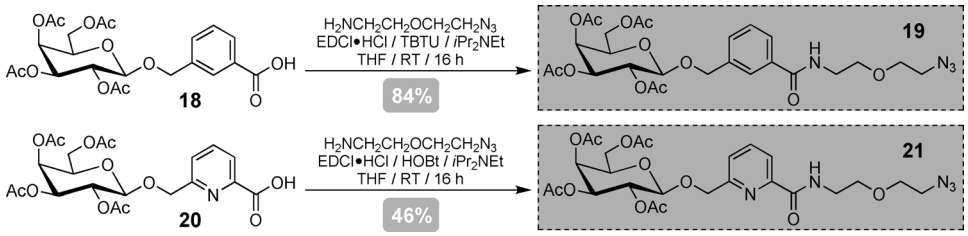

Scheme 4. Synthesis of the phenyl- and pyridine-based galactosides $GalPhEG_2N_3$ (**19**) and $GalPyrEG_2N_3$ (**21**; Pyr = pyridyl).

performed by using a peracetate galactosyl donor to the corresponding galactoside **15**. Concomitant saponification of both acetate protecting groups and the methyl ester followed by re-acetylation of the crude product provided carboxylic acid **16**. Condensation with 2-(2-azidoethoxy)ethanamine afforded amide **17** in good yield.

The previously reported[56] galactosides **18** and **20** were conjugated with 2-(2-azidoethoxy)ethanamine and provided amides **19** and **21**, respectively (Scheme 4). The pyridine derivative **21** was obtained in lower yields due to difficulty in purifying carboxylic acid **20**, the purity of which greatly alters the outcome of the amide-bond formation.

Tyrosine (Tyr) was used as a linker arm through either the amine or carboxylic acid moiety (Scheme 5). The carboxylic acid of Fmoc-tyrosine **22** was conjugated with 2-(2-azidoethoxy)ethanamine to the corresponding amide **23**. Galactosylation of the phenol moiety of tyrosine has been reported with galactosyl bromides[57,58] or trichloroacetimidates[59] as donors, but the readily available galactose peracetate[60,61] was used and provided the best yields. The glycosylation reaction proceeded under rather simple reaction conditions relative to previous results by using more sophisticated galactosyl donors.[57–59] Galactoside **24** was obtained in good yield (64%). Meanwhile, acid **22** was esterified to form allyl ester **25** and then galactosylated to the intermediate **26** in high yield (90%). A one-pot three-step process afforded the azido-functionalized intermediate **27** and removal of the allyl ester moiety led to the desired galactoside **28**.

Conjugation with oligonucleotides

The azido-functionalized CPG precursor **29**[62] was conjugated with propargyl α-D-mannopyranoside **30** in a Cu^I-catalyzed azide–alkyne cycloaddition reaction (CuAAC) on a solid support by using our standard methodology[63] (Scheme 6). The four hydroxy groups of the mannose moiety were converted into phosphitetriesters with phosphoramidites **32**–**34**.[38,46,64] Subsequent oxidation with iodine/water afforded phosphotriester linkages. Subsequent release of the dimethoxytrityl (DMTr) at the primary hydroxy function of the solid support allowed for elongation of a 15-mer oligonucleotide sequence and Cy3 labeling (see the Supporting Information). Treatment with am-

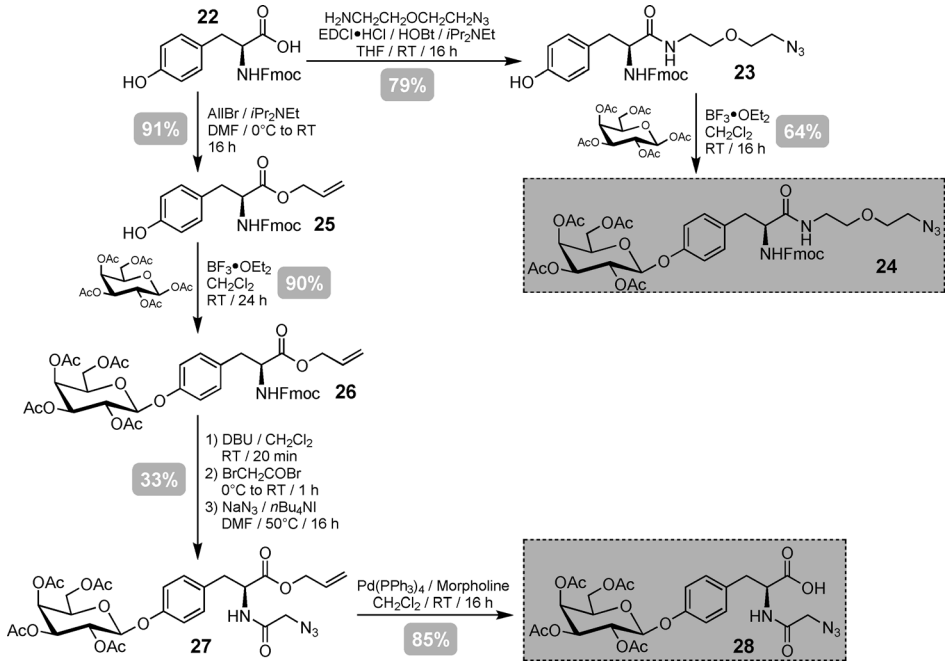

Scheme 5. Synthesis of the tyrosine-based galactosides $GalTyrEG_2N_3$ (**24**) and GalTyrNAz (**28**). Fmoc = 9-fluorenylmethoxycarbonyl.

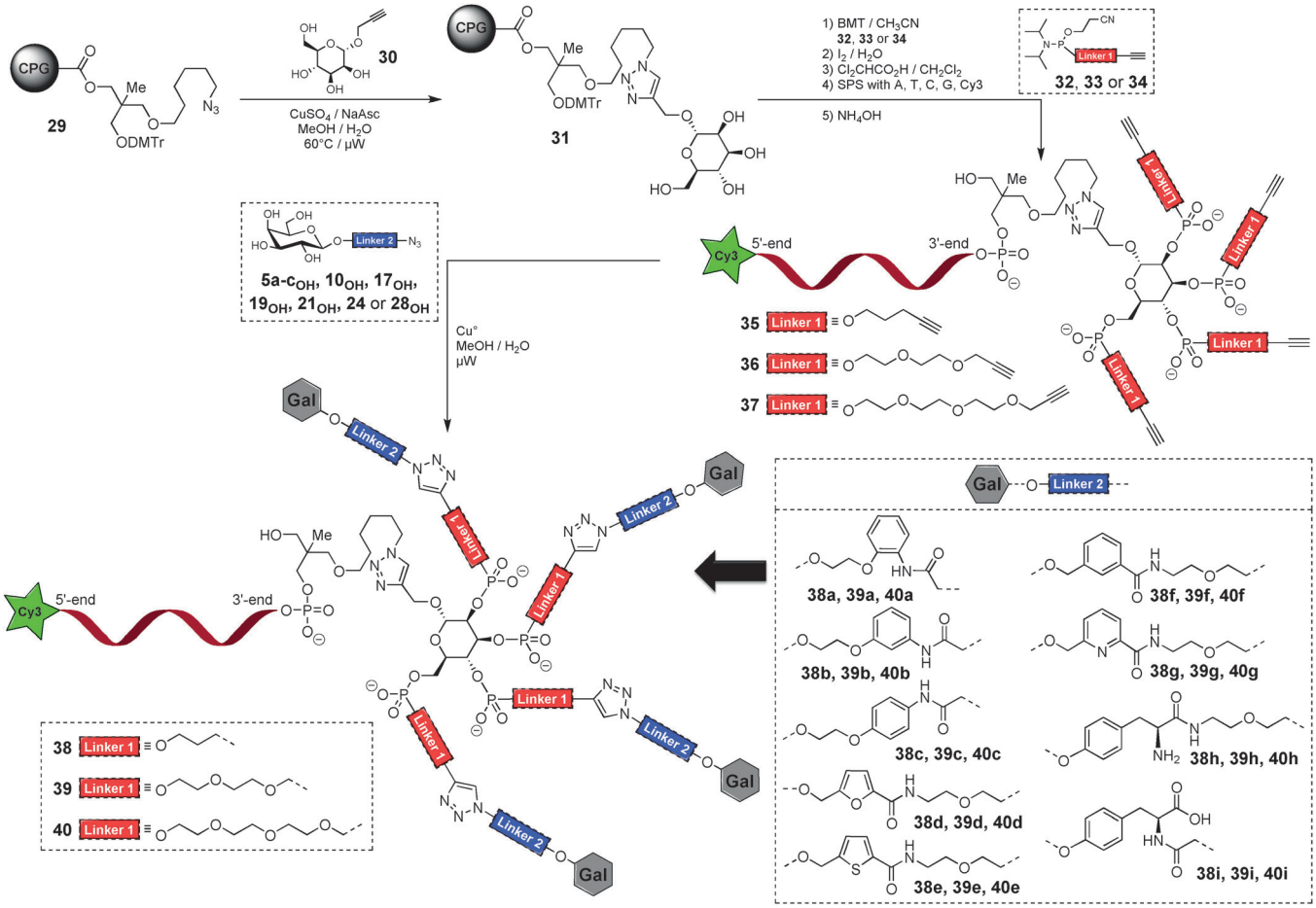

Scheme 6. Conjugation of azido-functionalized carbohydrate epitopes with the tetrapropargylated oligonucleotide-based scaffolds. Asc = ascorbate, BMT = 5-(benzylmercapto)-1*H*-tetrazole, CPG = controlled pore glass, DMTr = 4,4′-dimethoxytrityl, SPS = solid phase synthesis, A, T, C, G = protected nucleoside phosphoramidites of deoxyadenosine (A), deoxythymidine (T), deoxycytidine (C) and deoxyguanosine (G).

monia was used for cleavage from the CPG solid support and concomitant oligonucleotide deprotection to afford the Cy3-DNA tagged tetra-propargylated scaffolds **35**–**37**.

A second CuAAC conjugation to introduce the four galactoside moieties was performed in solution with the deprotected carbohydrates **5a**–$\mathbf{c_{OH}}$, $\mathbf{10_{OH}}$, $\mathbf{17_{OH}}$, $\mathbf{19_{OH}}$, $\mathbf{21_{OH}}$, and $\mathbf{28_{OH}}$ or the protected galactoside **24**. Deacetylation was performed by using the classic treatment of MeOH/Et_3N/H_2O. These hydroxylated carbohydrates were characterized by means of high-resolution mass spectrometric analysis (see Table S1 in the Supporting Information). Conjugations were initially performed in water according to our previously established protocol[45] by using a copper(0) species with microwave assistance for 1.5 hours at 65 °C (see Method A in the Supporting Information). Tris(benzyltriazolylmethyl)amine (TBTA) in methanol was used as a ligand for a copper(I) species that is known to accelerate the CuAAC[65] reaction, which was completed within 1 hour at room temperature (see Method B in the Supporting Information). Finally, tris(3-hydroxypropyl triazolylmethyl)-amine[66] (THPTA) was used instead of TBTA, and the reaction was performed in water with the same efficiency (see Method C in the Supporting Information). Therefore, glycoclusters **38**–**40** were obtained with variations in the three different linker arms at the phosphotriester site (**Linker 1**) and no less than nine structurally different spacer arms between the triazole and galactose moieties (**Linker 2**; Scheme 6).

Binding studies with microarrays

The 27 glycoclusters prepared were investigated for their binding properties toward the bacterial lectin LecA from *Pseudomonas aeruginosa*. First, the influence of **Linker 1** was assessed and the best type of **Linker 1** identified. The influence of different examples of **Linker 2** on the subfamily of nine glycoclusters, which incorporate the optimal **Linker 1**, was evaluated in a structure–activity relationships analysis. These investigations were first performed qualitatively by determining the fluorescence signals of LecA bound to the glycoclusters at the surface of the microarray and quantitatively by measuring the dissociation constants (K_d).

The glycocluster oligonucleotide conjugates were labeled with Cy3, whereas LecA was tagged with Alexa647. The Cy3 fluorescence signal monitored the relative surface densities of the different glycoclusters (less than 12% deviation). The Alexa647 fluorescence signal was used to monitor the binding of LecA with the glycoclusters (Figure 3).

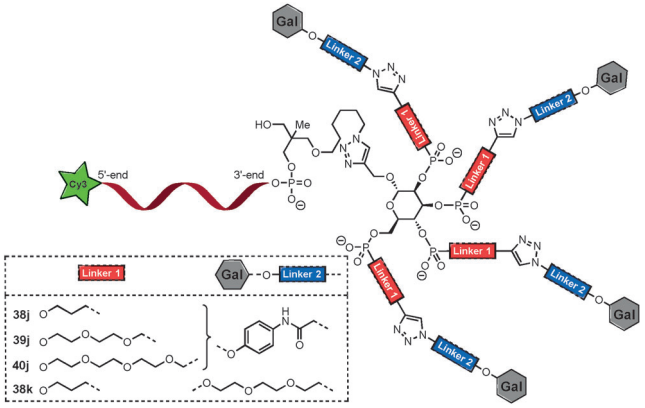

Figure 2. Structures of mannose-centered galactoclusters with aromatic or triethyleneglycol aglycons.

Aromatic aglycons drastically improve the binding of glycoclusters to LecA.[3,13,31,43,46,48–51] Three previously reported aromatic glycoclusters **38j**, **39j**, and **40j**[46] and glycocluster **38k**,[43] which does not possess an aromatic aglycon, but a triethyleneglycol linker, were also included in the study for comparison (Figure 2). Two negative controls were included in the microarray measurements. **TriMan**[47] (see the Supporting Information) displayed three mannose residues that should not interact with LecA. A second negative control (**ssDNA**) corresponded to a single-stranded DNA (Figure 3). The Alexa647 fluorescence signal was less than 56 AU for these negative controls, thus showing that no nonspecific binding occurred.

Influence of Linker 1

The influence of **Linker 1** was rather dependent on the nature of the aglycon with four different trends seen: 1) For the phenyl-based aglycons **a**–**c**, **f**, and **j**, the longer **Linker 1** (from propyl to triethyleneglycolmethylene, EG_3M) was, the better the affinity toward LecA. 2) For the furan-based (**d**) and $TyrNH_2$ (**h**) **Linker 1**, the opposite was observed. 3) However, no influence of **Linker 1** was observed for the $TyrCO_2H$ (**i**) aglycon. 4) Finally, a decrease of affinity from Pro to EG_2M, then an increase from Pro to EG_3M was observed for the thiophen- (**e**) and pyridine-based (**g**) aglycons. These observations are very difficult to rationalize, but the general trend (i.e., the longer that **Linker 1** is, the better the affinity for the lectin) is quite logical. This linker is internally positioned in the structure of the whole glycocluster and might moderately influence the binding properties toward LecA.

Influence of Linker 2

Linker **2** was introduced to probe the influence of 1) the regioisomery of the aromatic ring **a**–**c**, 2) the distance of this ring from the anomeric carbon atom of galactose (i.e., **a**–**c** versus **j**), and 3) the nature of the aromatic aglycon.

Among the 31 glycoclusters evaluated, the one moiety with a triethyleneglycol aglycon species (**Linker 2**) **38k** displayed the lowest affinity toward LecA.[43] This result confirmed the requirement of an aromatic aglycon to increase the affinity for LecA.

Glycoclusters that incorporate the *para*-substituted EG*para*-Ph (**c**), $TyrCO_2H$ (**i**), and *para*-Ph (**j**) moieties displayed, at a similar level, the best affinity for LecA. The next glycoclusters with a good affinity incorporated $TyrNH_2$ (**h**) and EG*meta*-Ph (**b**). Then, on the order of decreasing affinity are the thiophen-based (**e**), *meta*-Bn (**f**), furan-based (**d**), pyridine-based (**g**), and finally EG*ortho*-Ph (**a**) components. From the tested molecules, it appears that the influence of **Linker 2** was generally greater than the influence of **Linker 1**.

Glycoclusters **38a**–**c**, in which a flexible glycol (EG) chain was introduced between the anomeric center of the galactose residue and the aromatic ring, were compared. The *para*-substituted glycocluster **38c** provided the best binding properties

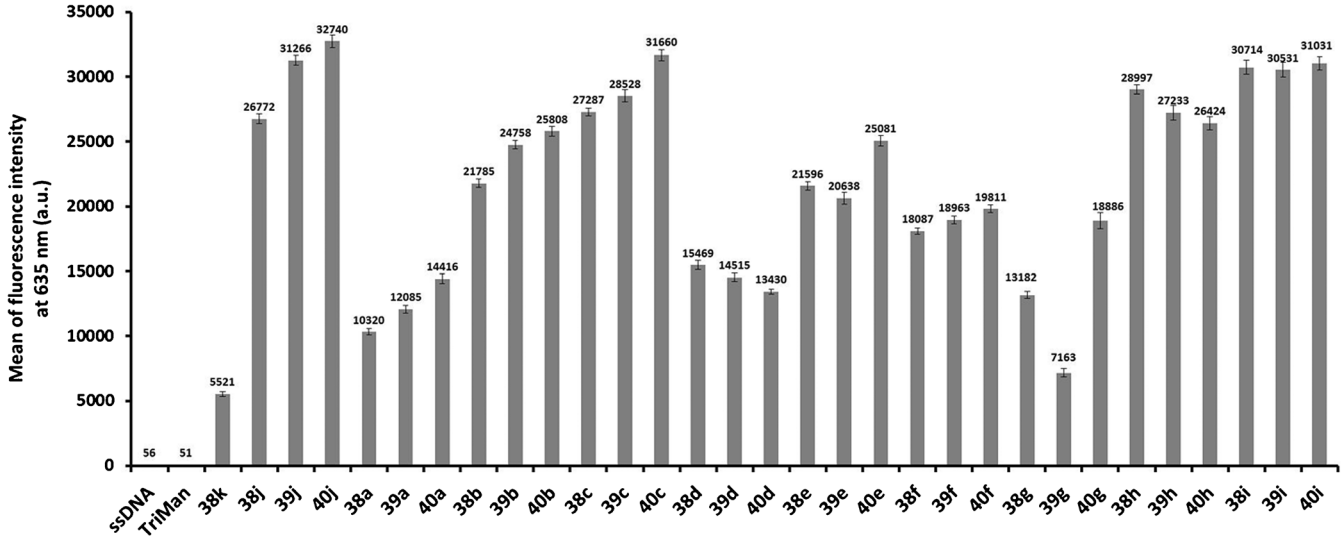

Figure 3. Alexa647–LecA fluorescence signal at $\lambda = 635$ nm as a function of the glycoclusters. The average value was calculated from 32 points per glycocluster.

toward LecA, better than the *meta*-regioisomer **38b**, whereas the *ortho*-derivative **38a** was mostly detrimental to the binding properties. The same influence was observed for the EG_2M **39** and EG_3M **40** species in the **Linker 1** series. The *ortho*-substitution pattern (**a**) probably generates significant steric hindrance because the amino acids of LecA are close to the carbohydrate-recognition domain. This effect is probably less important for the *meta*-regioisomer (**b**), whereas while the *para*-substituted derivative (**c**) is the least congested, thus providing the best affinity observed.

Finally, a comparison of **Linker 2** in the series of **d**–**g** provides insight to the influence of the aromatic ring. In this case, the order of influence within the glycoclusters was observed to be thiophen (**e**) > *meta*-Bn (**f**) > furan (**d**) > pyridine (**g**). The pyridine-based (**g**) **Linker 2** was superior among these four congeners only in the case of glycocluster **40**, and then it was only superior to the furan-based (**d**) **Linker 2**.

Measurements of dissociation constants (K_d) on microarrays

To gain a better understanding of the influence of **Linker 2**, dissociation constants (K_d) were measured by means of microarray to provide quantitative insight into the glycocluster-binding properties toward LecA (Table 2). The K_d values were determined only for the EG_3M (**40**) **Linker 1** series, which had been identified as the optimal linker for this position in the macromolecule. The quantitative K_d values (Table 2) were in agreement with the qualitative data obtained by direct fluorescence (Figure 3).

Table 2. Dissociation constants (K_d) measured by carbohydrate microarray.

Glycocluster	Linker 2	K_d [nM]	Rank	R^2
40a	EG*ortho*-Ph	304	10	0.963
40b	EG*meta*-Ph	52	5	0.993
40c	EG*para*-Ph	39	3	0.996
40d	furanyl	202	8[a]	0.991
40e	thiophenyl	77	6[a]	0.997
40f	*meta*-Bn	81	6[a]	0.985
40g	pyridyl	197	8[a]	0.986
40h	$TyrNH_2$	47	4	0.995
40i	$TyrCO_2H$	19	1	0.994
40j	*para*-Ph	28[b]	2	–[c]

[a] Could not be distinguished because the root-square deviation (RSD) of the K_d measurements determined by means of microarrays was less than 8%.[67] [b] The K_d value previously reported.[46] [c] Does not apply.

The preference in the substitution pattern at the phenyl ring was confirmed to be *para* (**c**) > *meta* (**b**) ≫ *ortho* (**a**). Indeed, the K_d values decreased by nearly sixfold between the *ortho* and *meta* isomers and by nearly eightfold between the *ortho* and *para* isomers.

A comparison between **40c** and **40j** showed that the introduction of an ethyleneglycol group between the galactose and phenyl rings had only a limited and small negative effect on the affinity (K_d = 39 and 28 nM, respectively).

The influence of the aromatic moiety was also confirmed. Glycoclusters **40** with a furanyl (**d**) or pyridinyl (**g**) ring exhibited the weakest binding with K_d values of around 200 nM, whereas those glycoclusters with thiophenyl (**e**) or *meta*-benzyl (**f**) groups exhibited better affinities with K_d values of around 80 nM, but were still about seven- and threefold less potent, respectively, than glycocluster **40j** with a phenyl linker (K_d = 28 nM).

As the stabilisation involves a face-to-edge π–π interaction between the ring and His50 of LecA, this interaction might be improved in the case of the thiophenyl (**e**) moiety based on the higher aromaticity due to the lower electronegativity of the sulfur atom relative to the oxygen atom in the furanyl ring (**d**). Furthermore, the addition of a methylene moiety on going from the *para*-Ph (**j**) to the *meta*-Bn (**f**) groups was detrimental, probably because the oxygen atom provides an enrichment in electron density on the aromatic ring of **40j**, which is beneficial for a better face-to-edge π–π interaction with the His50 residue.

Reymond and co-workers[13] reported that an amine group (as a lysine residue of the core moiety of the peptide-based glycocluster) close to the aromatic moiety can interact with the aspartic acid (Asp) residue Asp47 of LecA, thus leading to stabilization of the interaction through coulombic forces. In our case, the free amine group of the $TyrNH_2$-based glycocluster **40h** did not improve the binding relative to glycocluster **40j** (K_d = 47 and 28 nM, respectively). In contrast, the introduction of a carboxylic acid group into the $TyrCO_2H$-based glycocluster **40i** led to the best binding with a K_d value of 19 nM, thus being the best LecA ligand identified to date by using microarrays.

Molecular simulations

Investigations were performed by using molecular-simulation studies to rationalize the binding properties observed on the microarrays and their implications in the binding of the galactosides and their aglycons in the binding site of LecA. The stoichiometry typically observed in such mannose-centered glycoclusters with LecA was measured as $n = 0.5$.[14] The calculations were performed by considering that two branches of the same glycocluster would interact simultaneously with two binding sites of the same LecA tetramer.

Glycoclusters **40c**, **40h**, and **40i** (Figures 4–6) were investigated by using molecular simulations and docking techniques. Glycocluster **40c** was selected to evaluate the influence of the ethyleneglycol moiety introduced at the anomeric center upon binding to LecA. Glycoclusters **40h** and **40i** provided the best binding properties from the K_d measurements and were therefore further investigated. Because the high affinities observed point toward chelate-binding modes as previously observed for this lectin,[21,31,50] an empirical calculation of the potential energy of interaction ΔE was carried out for the six different possible combinations for the simultaneous binding of the two galactose epitopes displayed at the tip of two branches attached at the core mannopyranoside ring (Table 3).

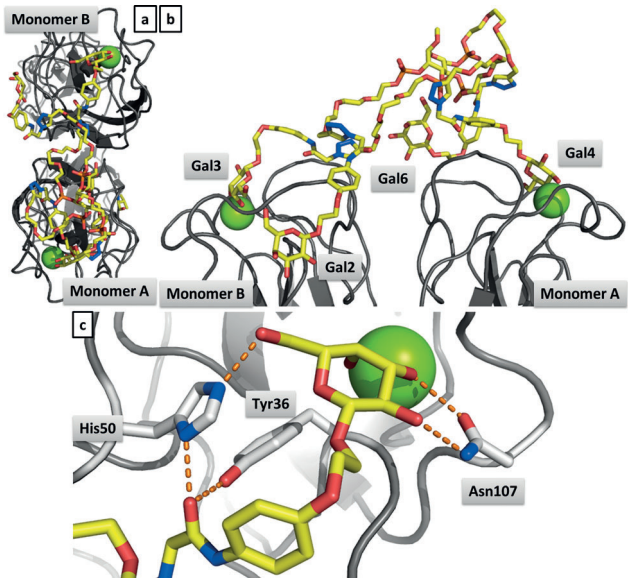

Figure 4. Glycocluster **40c** interacting with LecA. a) Top view, b) side view, c) binding-site close-up view of the O3 galactose residue. Calcium cations are represented as spheres. **Gal2**, **Gal3**, **Gal4**, and **Gal6** are the galactose epitopes displayed at the end of each linker arm of the mannopyranoside hydroxy groups. Dashed lines represent the hydrogen-bonding contacts.

A good ΔE-to-K_d correlation was observed for glycocluster **40c** with branches at the O3 and O4 atoms of the mannopyranoside ring ($K_d = 39$ nM, $\Delta E = -239$ kcal mol^{-1}). The galactoside epitope at position 3 interacts with the lectin monomer B through hydrogen bonds with the Tyr36, His50, and Asn107 residues (Figure 4c; Asn = asparagine). The His50 residue usually involved in CH–π stacking with other aromatic aglycons[13,48] now interacts with the OH-6 group of the galactose residue and the carbonyl bond of the amide group present on the aglycon. The same carbonyl bond also interacts with the Tyr36 residue. The O4 branch is only connected to monomer A through hydrogen bonds with the Thr39 and His50 residues. Furthermore, the His58 residue from the B monomer is in hydrogen-bond contact with the O2 branch. Finally, branch O6 also interacts with both monomers with hydrogen bonds formed toward the His50A, Glu49A, and Gln40B residues (Glu = glutamic acid, Gln = glutamine).

Glycocluster **40h** with a tyrosine–amine aglycon provided another good ΔE-to-K_d correlation when considering branches from positions 3 and 4 ($K_d = 47$ nM, $\Delta E = -232$ kcal mol^{-1}). The galactoside epitopes displayed on branches at positions 3 and 4 interact in the LecA binding site through the usual interactions, and no additional intermolecular bonding was observed (Figure 5). The remaining stabilizing interactions could be accounted for by the interaction of branches 2 and 6 with other parts of the glycocluster itself (if considering that these branches would not interact with another LecA tetramer in solution). The O3 galactoside interacts with the lectin monomer B through hydrogen bonds with the His50 residue, which again does not interact with the aromatic moiety but the 6-OH group of the galactose moiety (Figure 5c). Nevertheless, a van der Waals contact between the aromatic aglycon and the γ-proton of the proline residue Pro38 could be identified with a distance from 2.70 to 3.85 Å (Figure 5c). The amine group was not engaged in any electrostatic interaction with the protein.

Glycocluster **40i** with a tyrosinyl carboxylate group led to the most stable complex, in agreement with the lowest K_d value measured (19 nM). A good ΔE-to-K_d agreement was found with branches issued from positions 2 and 4 of the mannopyranoside ring ($K_d = 19$ nM, $\Delta E = -308$ kcal mol^{-1}). The galactose epitope at the O2 branch interacts with monomer B of the tetrameric lectin (Figure 6). The carboxylate group in the tyrosine-based linker is essentially exposed to the solvent, but also creates additional interactions with the Pro38 and Glu39 amino acids. The O4 branch interacts with monomer A of the same tetrameric lectin. The carboxylate group present in the linker is again engaged in a hydrogen bond with the His50 residue (Figure 6c). The TyrCO_2H aglycon therefore causes the de-

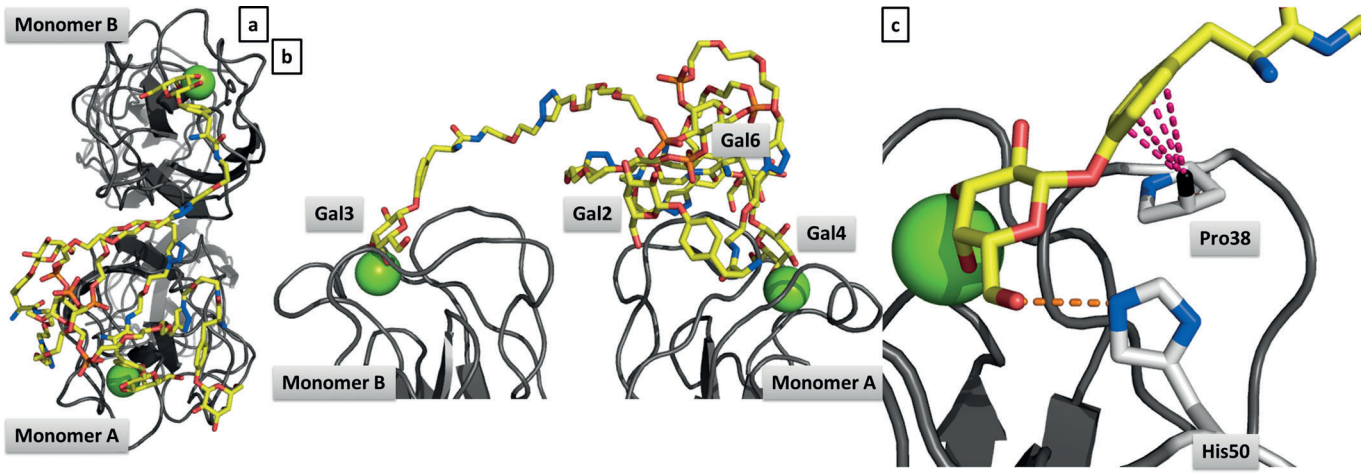

Figure 5. Glycocluster **40h** interacting with LecA. a) Top view, b) side view, c) binding-site close-up view of the O3 galactose residue. Calcium cations are represented as spheres. **Gal2**, **Gal3**, **Gal4**, and **Gal6** are the galactose epitopes displayed at the end of each linker arm of the mannopyranoside hydroxy groups. Dashed lines represent hydrogen-bonding contacts and also distances for the van der Waals interactions with Pro38.

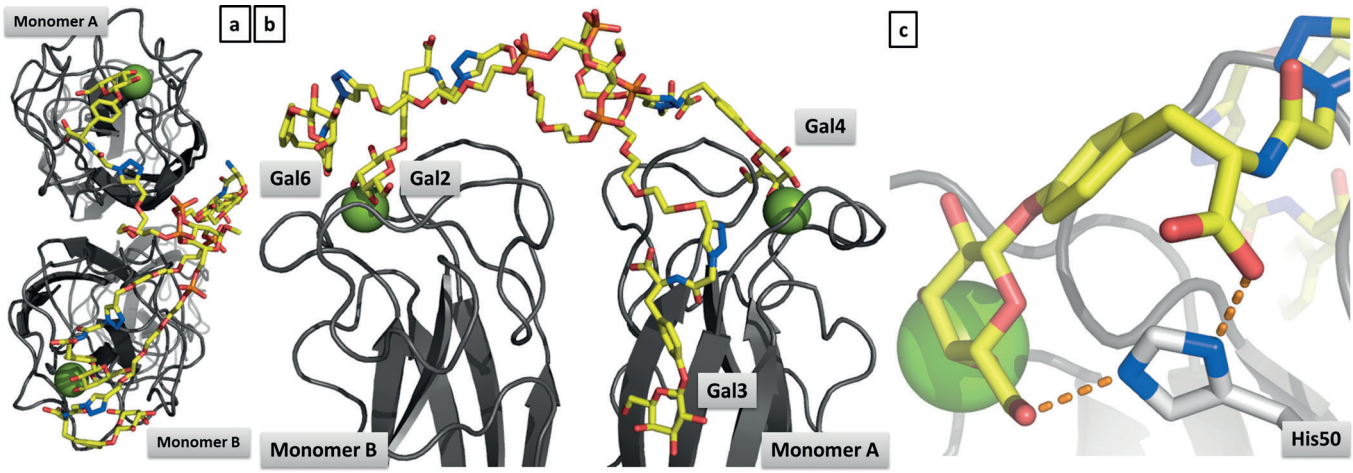

Figure 6. Glycocluster **40 i** interacting with LecA. a) Top view, b) side view, c) binding-site close-up view of the O4 galactose residue. Calcium cations are represented as spheres. **Gal2**, **Gal3**, **Gal4**, and **Gal6** are the galactose epitopes displayed at the end of each linker arm of the mannopyranoside hydroxy groups. Dashed lines represent hydrogen-bonding contacts.

Table 3. Empirical potential energy of interaction (ΔE) calculated from each possible two-set of branches from the mannopyranoside scaffold used for docking.

Glycocluster	Branches[a]						Mean[b]
	2–3	2–4	2–6	3–4	3–6	4–6	[kcal mol^{-1}]
40 c	−187	−215	−226	−239	−197	−170	−206
40 h	−199	−220	−236	−232	−259	−192	−223
40 i	−314	−308	−289	−174	−148	−303	−256

[a] Branches used for the dual docking from the mannopyranoside scaffold. The numbers used refer to the positions on the pyranose ring. [b] Average ΔE values for all the possible combinations of the branches.

viation of the His50 residue from the previously reported T-shaped CH–π interaction observed in the crystal structure toward an ionic interaction of the carboxylate group with the imidazole side chain. This ionic interaction is more energetically efficient than the CH–π contact, thus explaining the improved affinity measured.

Conclusions

LecA-targeting glycoclusters have been extensively studied, and the design of potent ligands of this lectin is of prime interest in antiadhesive therapies against infection by *Pseudomonas aeruginosa*. The binding properties of these ligands have been improved by using aromatic aglycons (typically *O*-phenyl galactosides). A family of 27 glycoclusters was synthesized with a combination of two linker arms that connect the central mannopyranoside core to the galactoside moieties. Aromatic aglycons, such as phenyl, furanyl, thiophenyl, pyridyl, or tyrosinyl groups, were investigated and a low-nanomolar (K_d = 19 nM) ligand with a tyrosine-based linker arm was identified in a structure–activity relationship study. The role of the lectin amino acid side chains in the binding of the three best glycoclusters was studied by using molecular modeling to rationalize the binding properties observed. The glycocluster that incorporated the tyrosine-based linker arm appears to be a new "lead" for the design of potential anti-infectious agents against *Pseudomonas aeruginosa* lung infection.

Acknowledgements

This project was supported by the *Agence Nationale de la Recherche* (Glycomime project ANR-12-BSV5-0020). The authors thank the Université Claude Bernard Lyon 1, Ecole Centrale de Lyon, Université Lille 1, Université de Montpellier and the CNRS for financial support. F.M. is from Inserm. Dr. R. Simon and C. Duchamp are gratefully acknowledged for the mass-spectrometric analyses.

Keywords: glycoclusters · microarrays · multivalency · oligonucleotides · *Pseudomonas aeruginosa*

[1] C. A. Bewley, *Protein–Carbohydrate Interactions in Infectious Diseases*, RSC, Cambridge, **2006**.
[2] Y. M. Chabre, R. Roy, *Chem. Soc. Rev.* **2013**, *42*, 4657–4708.
[3] S. Cecioni, A. Imberty, S. Vidal, *Chem. Rev.* **2015**, *115*, 525–561.
[4] D. Abgottspon, B. Ernst, *Chimia* **2012**, *66*, 166–169.
[5] C. K. Cusumano, J. S. Pinkner, Z. Han, S. E. Greene, B. A. Ford, J. R. Crowley, J. P. Henderson, J. W. Janetka, S. J. Hultgren, *Sci. Transl. Med.* **2011**, *3*, 109ra115.
[6] Z. Han, J. S. Pinkner, B. Ford, E. Chorell, J. M. Crowley, C. K. Cusumano, S. Campbell, J. P. Henderson, S. J. Hultgren, J. W. Janetka, *J. Med. Chem.* **2012**, *55*, 3945–3959.
[7] M. Totsika, M. Kostakioti, T. J. Hannan, M. Upton, S. A. Beatson, J. W. Janetka, S. J. Hultgren, M. A. Schembri, *J. Infect. Dis.* **2013**, *208*, 921–928.
[8] S. Vanwetswinkel, A. N. Volkov, Y. G. J. Sterckx, A. Garcia-Pino, L. Buts, W. F. Vranken, J. Bouckaert, R. Roy, L. Wyns, N. A. J. van Nuland, *J. Med. Chem.* **2014**, *57*, 1416–1427.
[9] A. M. Boukerb, A. Rousset, N. Galanos, J.-B. Méar, M. Thépaut, T. Grandjean, E. Gillon, S. Cecioni, C. Abderrahmen, K. Faure, D. Redelberger, E. Kipnis, R. Dessein, S. Havet, B. Darblade, S. E. Matthews, S. de Bentzmann, B. Guéry, B. Cournoyer, A. Imberty, S. Vidal, *J. Med. Chem.* **2014**, *57*, 10275–10289.
[10] C. Chemani, A. Imberty, S. de Bentzman, P. Pierre, M. Wimmerová, B. P. Guery, K. Faure, *Infect. Immun.* **2009**, *77*, 2065–2075.
[11] H.-P. Hauber, M. Schulz, A. Pforte, D. Mack, P. Zabel, U. Schumacher, *Int. J. Med. Sci.* **2008**, *5*, 371–376.

[12] E. M. V. Johansson, S. A. Crusz, E. Kolomiets, L. Buts, R. U. Kadam, M. Cacciarini, K.-M. Bartels, S. P. Diggle, M. Cámara, P. Williams, R. Loris, C. Nativi, F. Rosenau, K.-E. Jaeger, T. Darbre, J.-L. Reymond, *Chem. Biol.* **2008**, *15*, 1249 – 1257.
[13] R. U. Kadam, M. Bergmann, M. Hurley, D. Garg, M. Cacciarini, M. A. Swiderska, C. Nativi, M. Sattler, A. R. Smyth, P. Williams, M. Cámara, A. Stocker, T. Darbre, J.-L. Reymond, *Angew. Chem. Int. Ed.* **2011**, *50*, 10631 – 10635; *Angew. Chem.* **2011**, *123*, 10819 – 10823.
[14] C. Ligeour, O. Vidal, L. Dupin, F. Casoni, E. Gillon, A. Meyer, S. Vidal, G. Vergoten, J.-M. Lacroix, E. Souteyrand, A. Imberty, J.-J. Vasseur, Y. Chevolot, F. Morvan, *Org. Biomol. Chem.* **2015**, *13*, 8433 – 8444.
[15] A. Imberty, M. Wimmerová, C. Sabin, E. P. Mitchell, *Structures and Roles of Pseudomonas Aeruginosa Lectins, in Protein – Carbohydrate Interactions in Infectious Diseases* (Ed.: C. A. Bewley), RSC Biomolecular Sciences, Cambridge, **2006**, Chapter 3, pp. 30 – 48.
[16] G. Cioci, E. P. Mitchell, C. Gautier, M. Wimmerova, D. Sudakevitz, S. Pérez, N. Gilboa-Garber, A. Imberty, *FEBS Lett.* **2003**, *555*, 297 – 301.
[17] E. Mitchell, C. Houles, D. Sudakevitz, M. Wimmerova, C. Gautier, S. Pérez, A. M. Wu, N. Gilboa-Garber, A. Imberty, *Nat. Struct. Biol.* **2002**, *9*, 918 – 921.
[18] D. Deniaud, K. Julienne, S. G. Gouin, *Org. Biomol. Chem.* **2011**, *9*, 966 – 979.
[19] S. Cecioni, S. Faure, U. Darbost, I. Bonnamour, H. Parrot-Lopez, O. Roy, C. Taillefumier, M. Wimmerová, J.-P. Praly, A. Imberty, S. Vidal, *Chem. Eur. J.* **2011**, *17*, 2146 – 2159.
[20] Y. Chen, H. Vedala, G. P. Kotchey, A. Audfray, S. Cecioni, A. Imberty, S. Vidal, A. Star, *ACS Nano* **2012**, *6*, 760 – 770.
[21] D. Sicard, S. Cecioni, M. Iazykov, Y. Chevolot, S. E. Matthews, J.-P. Praly, E. Souteyrand, A. Imberty, S. Vidal, M. Phaner-Goutorbe, *Chem. Commun.* **2011**, *47*, 9483 – 9485.
[22] H. Vedala, Y. Chen, S. Cecioni, A. Imberty, S. Vidal, A. Star, *Nano Lett.* **2011**, *11*, 170 – 175.
[23] D. Sicard, Y. Chevolot, E. Souteyrand, A. Imberty, S. Vidal, M. Phaner-Goutorbe, *J. Mol. Recognit.* **2013**, *26*, 694 – 699.
[24] S. Cecioni, V. Oerthel, J. Iehl, M. Holler, D. Goyard, J.-P. Praly, A. Imberty, J.-F. Nierengarten, S. Vidal, *Chem. Eur. J.* **2011**, *17*, 3252 – 3261.
[25] J.-F. Nierengarten, J. Iehl, V. Oerthel, M. Holler, B. M. Illescas, A. Munoz, N. Martin, J. Rojo, M. Sanchez-Navarro, S. Cecioni, S. Vidal, K. Buffet, M. Durka, S. P. Vincent, *Chem. Commun.* **2010**, *46*, 3860 – 3862.
[26] M. Durka, K. Buffet, J. Iehl, M. Holler, J.-F. Nierengarten, J. Taganna, J. Bouckaert, S. P. Vincent, *Chem. Commun.* **2011**, *47*, 1321 – 1323.
[27] I. Nierengarten, J.-F. Nierengarten, *Chem. Asian J.* **2014**, *9*, 1436 – 1444.
[28] A. Muñoz, D. Sigwalt, B. M. Illescas, J. Luczkowiak, L. Rodríguez-Pérez, I. Nierengarten, M. Holler, J.-S. Remy, K. Buffet, S. P. Vincent, J. Rojo, R. Delgado, J.-F. Nierengarten, N. Martín, *Nat. Chem.* **2016**, *8*, 50 – 57.
[29] S. Cecioni, O.-A. Argintaru, T. Docsa, P. Gergely, J.-P. Praly, S. Vidal, *New J. Chem.* **2009**, *33*, 148 – 156.
[30] S. Cecioni, S. E. Matthews, H. Blanchard, J.-P. Praly, A. Imberty, S. Vidal, *Carbohydr. Res.* **2012**, *356*, 132 – 141.
[31] S. Cecioni, J.-P. Praly, S. E. Matthews, M. Wimmerová, A. Imberty, S. Vidal, *Chem. Eur. J.* **2012**, *18*, 6250 – 6263.
[32] A. Dondoni, A. Marra, *Chem. Rev.* **2010**, *110*, 4949 – 4977.
[33] S. P. Vincent, K. Buffet, I. Nierengarten, A. Imberty, J.-F. Nierengarten, *Chem. Eur. J.* **2016**, *22*, 88 – 92.
[34] G. Yu, Y. Ma, C. Han, Y. Yao, G. Tang, Z. Mao, C. Gao, F. Huang, *J. Am. Chem. Soc.* **2013**, *135*, 10310 – 10313.
[35] I. Nierengarten, K. Buffet, M. Holler, S. P. Vincent, J.-F. Nierengarten, *Tetrahedron Lett.* **2013**, *54*, 2398 – 2402.
[36] K. Buffet, I. Nierengarten, N. Galanos, E. Gillon, M. Holler, A. Imberty, S. E. Matthews, S. Vidal, S. P. Vincent, J.-F. Nierengarten, *Chem. Eur. J.* **2016**, *22*, 2955 – 2963.
[37] N. Galanos, E. Gillon, A. Imberty, S. E. Matthews, S. Vidal, *Org. Biomol. Chem.* **2016**, *14*, 3476 – 3481.
[38] B. Gerland, A. Goudot, G. Pourceau, A. Meyer, V. Dugas, S. Cecioni, S. Vidal, E. Souteyrand, J.-J. Vasseur, Y. Chevolot, F. Morvan, *Bioconjugate Chem.* **2012**, *23*, 1534 – 1547.
[39] B. Gerland, A. Goudot, G. Pourceau, A. Meyer, S. Vidal, E. Souteyrand, J.-J. Vasseur, Y. Chevolot, F. Morvan, *J. Org. Chem.* **2012**, *77*, 7620 – 7626.
[40] F. Morvan, S. Vidal, E. Souteyrand, Y. Chevolot, J.-J. Vasseur, *RSC Adv.* **2012**, *2*, 12043 – 12068.
[41] A. Goudot, G. Pourceau, A. Meyer, T. Gehin, S. Vidal, J.-J. Vasseur, F. Morvan, E. Souteyrand, Y. Chevolot, *Biosens. Bioelectron.* **2013**, *40*, 153 – 160.
[42] C. Ligeour, A. Audfray, E. Gillon, A. Meyer, N. Galanos, S. Vidal, J.-J. Vasseur, A. Imberty, F. Morvan, *RSC Adv.* **2013**, *3*, 19515 – 19524.
[43] B. Gerland, A. Goudot, C. Ligeour, G. Pourceau, A. Meyer, S. Vidal, T. Gehin, O. Vidal, E. Souteyrand, J.-J. Vasseur, Y. Chevolot, F. Morvan, *Bioconjugate Chem.* **2014**, *25*, 379 – 392.
[44] C. Ligeour, L. Dupin, A. Angeli, G. Vergoten, S. Vidal, A. Meyer, E. Souteyrand, J.-J. Vasseur, Y. Chevolot, F. Morvan, *Org. Biomol. Chem.* **2015**, *13*, 11244 – 11254.
[45] G. Pourceau, A. Meyer, Y. Chevolot, E. Souteyrand, J. J. Vasseur, F. Morvan, *Bioconjugate Chem.* **2010**, *21*, 1520 – 1529.
[46] F. Casoni, L. Dupin, G. Vergoten, A. Meyer, C. Ligeour, T. Gehin, O. Vidal, E. Souteyrand, J.-J. Vasseur, Y. Chevolot, F. Morvan, *Org. Biomol. Chem.* **2014**, *12*, 9166 – 9179.
[47] Y. Chevolot, C. Bouillon, S. Vidal, F. Morvan, A. Meyer, J.-P. Cloarec, A. Jochum, J.-P. Praly, J.-J. Vasseur, E. Souteyrand, *Angew. Chem. Int. Ed.* **2007**, *46*, 2398 – 2402; *Angew. Chem.* **2007**, *119*, 2450 – 2454.
[48] R. U. Kadam, D. Garg, J. Schwartz, R. Visini, M. Sattler, A. Stocker, T. Darbre, J. L. Reymond, *ACS Chem. Biol.* **2013**, *8*, 1925 – 1930.
[49] J. Rodrigue, G. Ganne, B. Blanchard, C. Saucier, D. Giguère, T. C. Shiao, A. Varrot, A. Imberty, R. Roy, *Org. Biomol. Chem.* **2013**, *11*, 6906 – 6918.
[50] M. L. Gening, D. V. Titov, S. Cecioni, A. Audfray, A. G. Gerbst, Y. E. Tsvetkov, V. B. Krylov, A. Imberty, N. E. Nifantiev, S. Vidal, *Chem. Eur. J.* **2013**, *19*, 9272 – 9285.
[51] Y. M. Chabre, D. Giguère, B. Blanchard, J. Rodrigue, S. Rocheleau, M. Neault, S. Rauthu, A. Papadopoulos, A. A. Arnold, A. Imberty, R. Roy, *Chem. Eur. J.* **2011**, *17*, 6545 – 6562.
[52] L. Fumagalli, C. Bolchi, S. Colleoni, M. Gobbi, B. Moroni, M. Pallavicini, A. Pedretti, L. Villa, G. Vistoli, E. Valoti, *Bioorg. Med. Chem.* **2005**, *13*, 2547 – 2559.
[53] P. K. Hashim, R. Thomas, N. Tamaoki, *Chem. Eur. J.* **2011**, *17*, 7304 – 7312.
[54] W. H. Steel, F. Damkaci, R. Nolan, R. A. Walker, *J. Am. Chem. Soc.* **2002**, *124*, 4824 – 4831.
[55] A. Boyer, M. Lautens, *Angew. Chem. Int. Ed.* **2011**, *50*, 7346 – 7349; *Angew. Chem.* **2011**, *123*, 7484 – 7487.
[56] S. Wang, J. A. Cuesta-Seijo, D. Lafont, M. M. Palcic, S. Vidal, *Chem. Eur. J.* **2013**, *19*, 15346 – 15357.
[57] F. Arena, J. B. Singh, E. Gianolio, R. Stefania, S. Aime, *Bioconjugate Chem.* **2011**, *22*, 2625 – 2635.
[58] A. Vargas-Berenguel, M. Meldal, H. Paulsen, K. J. Jensen, K. Bock, *J. Chem. Soc. Perkin Trans. 1* **1994**, 3287 – 3294.
[59] N. E. Fahmi, L. Dedkova, B. Wang, S. Golovine, S. M. Hecht, *J. Am. Chem. Soc.* **2007**, *129*, 3586 – 3597.
[60] H. Lin, D. A. Thayer, C.-H. Wong, C. T. Walsh, *Chem. Biol.* **2004**, *11*, 1635 – 1642.
[61] N. Yao, G. Fung, H. Malekan, L. Ye, M. J. Kurth, K. S. Lam, *Carbohydr. Res.* **2010**, *345*, 2277 – 2281.
[62] G. Pourceau, A. Meyer, J.-J. Vasseur, F. Morvan, *J. Org. Chem.* **2009**, *74*, 6837 – 6842.
[63] C. Bouillon, A. Meyer, S. Vidal, A. Jochum, Y. Chevolot, J. P. Cloarec, J. P. Praly, J. J. Vasseur, F. Morvan, *J. Org. Chem.* **2006**, *71*, 4700 – 4702.
[64] A. Meyer, G. Pourceau, J. J. Vasseur, F. Morvan, *J. Org. Chem.* **2010**, *75*, 6689 – 6692.
[65] T. R. Chan, R. Hilgraf, K. B. Sharpless, V. V. Fokin, *Org. Lett.* **2004**, *6*, 2853 – 2855.
[66] V. Hong, S. I. Presolski, C. Ma, M. G. Finn, *Angew. Chem. Int. Ed.* **2009**, *48*, 9879 – 9883; *Angew. Chem.* **2009**, *121*, 10063 – 10067.
[67] L. Dupin, F. Zuttion, T. Gehin, A. Meyer, M. Phaner-Goutorbe, J. J. Vasseur, E. Souteyrand, F. Morvan, Y. Chevolot, *ChemBioChem* **2015**, *16*, 2329 – 2336.

Received: May 2, 2016
Published online on ■■ ■■, 0000

FULL PAPER

Sweet tyrosine: A series of 27 glycoclusters that target lectin A (LecA) have been synthesized. Aromatic aglycons, such as phenyl, furanyl, thiophenyl, pyridyl, or tyrosinyl, were investigated and a low-nanomolar (K_d = 19 nM) LecA ligand with a tyrosine-based linker arm was further investigated by molecular modelling (see figure; His = histidine).

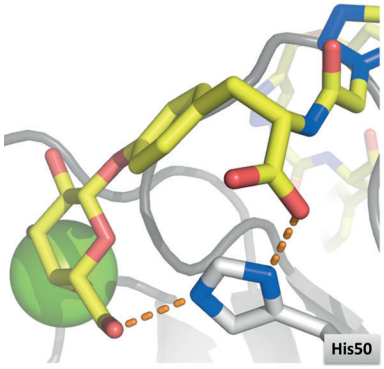

Glycoclusters

S. Wang, L. Dupin, M. Noël, C. J. Carroux, L. Renaud, T. Géhin, A. Meyer, E. Souteyrand, J.-J. Vasseur, G. Vergoten, Y. Chevolot, F. Morvan,* S. Vidal**

■■ – ■■

Toward the Rational Design of Galactosylated Glycoclusters That Target *Pseudomonas aeruginosa* Lectin A (LecA): Influence of Linker Arms That Lead to Low-Nanomolar Multivalent Ligands